# On the advanced microstructural characterisation of additively manufactured alumina-zirconia based eutectic ceramics

Mainak Saha[1,2]

[1]Department of Metallurgical and Materials Engineering, Indian Institute of Technology Madras, Chennai-600036

[2]Department of Metallurgical and Materials Engineering, National Institute of Technology Durgapur-713209

Corresponding author: Mainak Saha

Email address (es): mainaksaha1995@gmail.com

Phone number: +918017457062

ORCID: Mainak Saha: 0000-0001-8979-457x

## Abstract

Due to the exceptional creep and oxidation resistance as well as excellent microstructural stability of alumina-zirconia (Al2O3-ZrO2) based eutectic ceramics, there have been a number of reports on their fabrication using laser additive manufacturing (AM) techniques recently. Additionally, it has been reported that the change of process parameters, particularly the laser scanning speed, connected with the aforementioned AM processes, results in the formation of a variety of intriguing microstructural characteristics (in these materials). The current review article presents a summary of the current status of research in the field of laser AM AZ-based eutectic ceramics and emphasises the difficulties and prospects for this line of inquiry. Additionally, the outlooks section has emphasised the necessity of using correlative microstructural characterization in these materials.

**Keywords:** $Al_2O_3$-based eutectic ceramics, Additive Manufacturing, Scanning Transmission Electron Microscopy, Correlative characterisation.

## 1. Introduction

Given a number of advantageous characteristics, most notably low density, high compressive strength, wear resistance, electrical and thermal insulating capabilities, alumina (Al2O3)-based ceramics are widely used in industry [1]. Al2O3 ceramic is a possible contender for dental and orthopaedic applications due to its high-purity material's favourable compressive characteristics and biocompatibility [2]. The layer-by-layer deposition of materials used in laser additive manufacturing (AM) processes, on the other hand, causes large-scale microstructural heterogeneity and the development of cracks in the deposited layers as a resultof thermal stresses [3]–[12]. The material (to be deposited) must, however, have a good fracturetoughness in order to prevent crack formation during layerwise deposition [3], [13]-[16]. Al2O3 ceramics' main drawback is their low fracture toughness, which prevents laser-based AM techniques from being used on them [1].

Through crack bridging and deflection mechanisms, zirconia (ZrO2) addition to Al2O3 ceramics has been shown to be a successful method of increasing fracture toughness (in AM-based samples). The effects of ZrO2 addition to AM-based Al2O3 were described by Pappas et al. [1] utilising the laser direct deposition process. Li and Zhang [17] examined the microstructure of Al2O3-ZrO2 (AZ) ceramics produced using the laser direct deposition process and with ZrO2 concentrations greater than 35 weight percent. According to Wilkes et al. [18], AZ ceramics can be successfully made without microcracking by preheating each layer (using a CO2 laser beam). Homeny and Nick [19] have looked into the relationship between AZ-Y2O3 eutectic ceramic structure and properties. The stabilisation of ZrO2 lamella in rapidly formed AZ eutectic ceramic has been studied by Moreno and Yoshimura [20].

Through crack bridging and deflection mechanisms, zirconia (ZrO2) addition to Al2O3 ceramics has been shown to be a successful method of increasing fracture toughness (in AM-based samples). The effects of ZrO2 addition to AM-based Al2O3 were described by Pappas et al. [1] utilising the laser direct deposition process. Li and Zhang [17] examined the microstructure of Al2O3-ZrO2 (AZ) ceramics produced using the laser direct deposition process and with ZrO2 concentrations greater than 35 wt.%. Wilkes et al. [18] have reported that preheating of every layer (using a $CO_2$ laser beam) may be successfully employed to eliminate micro-cracking in AZ ceramics. Homeny and Nick [19] have investigated the structure-property correlation in AZ-$Y_2O_3$ eutectic ceramic. Moreno and Yoshimura [20] have investigated the stabilisation of $ZrO_2$ lamella in rapidly solidified AZ eutectic ceramic. The microstructure and physical characteristics of directionally solidified AZ eutectic ceramic have been studied by Trnovcova et al. [21]. By emphasising three recent investigations in the particular field, the current article aims to provide an overview of the current state of study in the area of laser AM AZ-based eutectic ceramics. At the end of the article, a brief future perspective in this direction has also been highlighted.

## 2. Relevant topics

### 2.1 Characterization of colonial boundaries in laser-directed energy deposition-fabricated AZ-GdAlO3 eutectic ceramic

The microstructure of an AZ-GdAlO3 eutectic ceramic made utilising the laser directed energy deposition (LDED) technology has been studied by Liu et al. [22]. Periodic banded formations have been shown to occur in the building direction (BD), and their emergence has been attributed to the aberrant growth of nanoscale features along the melt pool [22]. A "Chinese-script" eutectic structure with an entanglement of bright (GdAlO3) and dark phases (Al2O3) was discovered within a eutectic colony [22]. The longitudinal section of colonies was also found to have a columnar morphology and to be extended perpendicular to the BD [22]. The heat conduction behaviour in the melt pool, which causes the microstructural growth to occur against the heat flow, was primarily ascribed for the aforementioned shape of the colonies (along the longitudinal section).

Additionally, it was noted that the eutectic spacing decreased from ~ 0.63 ± 0.11 μm at the sample surface to ~ 0.99 ± 0.08 μm in the sample centre [22]. This has been explained by a faster rate of cooling at the surface than inside the sample [22]. Concave bands may be seen

along BD in Fig. 1(a). The colonial boundaries are clearly visible in the Scanning Electron Microscopy (SEM)-based microstructures in the various levels of the cladding layer shown in Figs. 1(b) through (d).

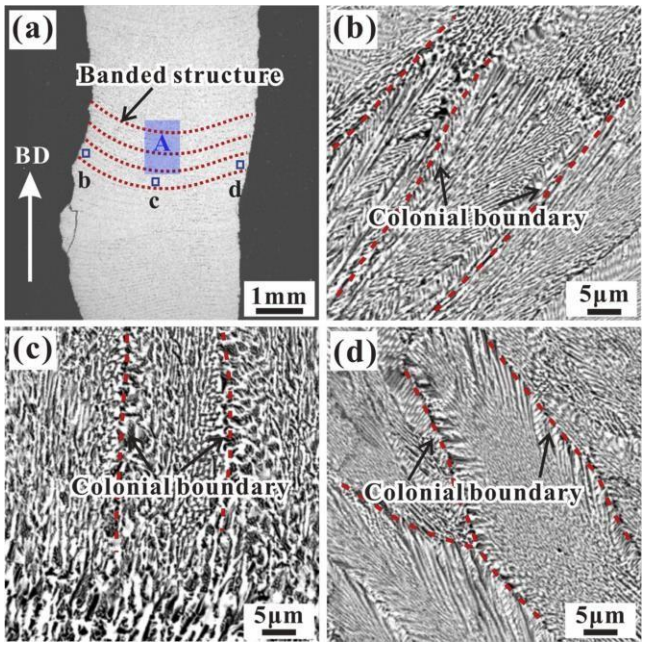


**Fig. 1** SEM micrographs (of the longitudinal section) of the AZ-$GdAlO_3$ eutectic ceramic: **(a)** periodic banded structure, **(b)** Left side of a deposited layer, **(c)** Centre of a deposited layer, and **(d)** Right side of a deposited layer [22].

### 2.2 Microstructure obtained during solidification of selective laser melted AZ-$GdAlO_3$ eutectic ceramic

The effect of laser scanning speed on the solidification of AZ-GdAlO3 eutectic ceramic during selective laser melting (SLM) technology has been studied by Liu et al. [23]. When the laser scanning speed was increased to 48 mm/min, it was found that the relative density of the solidified samples decreased from 98.7% to 95.7% [23]. A decrease in both melting width and depth was seen with an increase in scanning speed, which was further evidence that the principal heat transmission mechanism linked to the solidification process is thermal conduction [23].

A fascinating finding was that the eutectic spacing in the top zone of the melt pool increases with increasing laser scanning speed from 12 mm/min to 48 mm/min after initially decreasing with increasing laser scanning speed from 6 mm/min to 12 mm/min [23]. The previously noted relationship between eutectic spacing and scanning speed was explained by a switch in the factor governing the solidification rate from laser scanning speed to the angle between the scanning direction and the microstructure's growth direction [16], [23]. For scanning speeds of less than 12 mm/min, quenching was observed to cause microcracks and increased surface roughness (because to the bailing effect and the presence of microstructural pores) [23]. Additionally, laser scanning speeds of less than 12 mm/min were reported to decrease solidification defects [23].

### 2.3 Nanostructured AZ-YAG fabricated using laser engineered net shaping technique

Using the LENS process, Fan et al. [24] reported fabricating an extremely dense (98%) thin-walled Al2O3-YAG-ZrO2 (AYZ) eutectic ceramic. Three phases—namely, -Al2O3, YAG, and ZrO2—are interpenetrated in the material's as-synthesized condition and exhibit a cellular microstructure [24]. For every layer that was deposited, a morphological change from a planar to a cellular eutectic microstructure (along BD) was also noted [24]. A picture of AYZ ceramic in its as-fabricated state taken using scanning transmission electron microscopy (STEM) and high-angle annular dark field (HAADF) is shown in Fig. 2(a) [24]. The matching STEM-Energy Dispersive Spectroscopy (EDS) maps for Al, Y, Zr, and O are shown in Figs. 2(b-e). As is clear from Figs. 2(b-e) and Table. 1, the dark, grey, and brilliant phases in the STEM-HAADF image (Fig. 2(a)) correspond to the -Al2O3, YAG, and cubic ZrO2 phases, respectively. Additionally, it can be seen in Figs. 2(c-e) and Table. 1 that 18 mol% of Y2O3 is dissolved in ZrO2 in the as-fabricated condition, showing that cubic ZrO2 is stabilised by Y3+ during cooling and solidification (during LENS) [24].

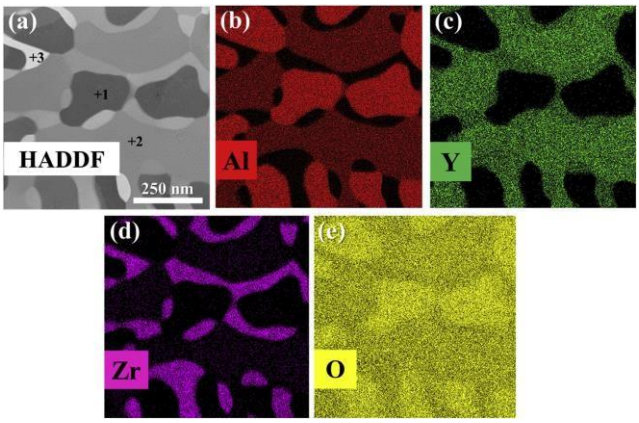


**Fig. 2** AYZ: **(a)** STEM-HAADF image, and corresponding STEM-EDS maps of **(b)** Al, **(c)** Y, **(d)** Zr, and **(e)** O [24]. Points 1, 2 and 3 marked in part **(a)** represent the regions where point EDS mapping has been performed. Results of point EDS mapping at points 1, 2 and 3 have been shown in **Table. 1**

**Table. 1** Composition (in at.%) at points 1, 2 and 3 obtained using point STEM-EDS analysis [24]

| Elements | 1 | 2 | 3 |
|---|---|---|---|
| **Al** | **35** | **22.5** | **1.3** |
| **Y** | **0** | **8.4** | **7.9** |
| **Zr** | **0** | **0.6** | **17.1** |
| **O** | **65** | **68.5** | **73.7** |

Along the boundary region of the manufactured specimens, it was also claimed that a fibrous eutectic structure interpenetrated irregularly [24]. This was explained by a significantly faster rate of solidification at the boundary region compared to the interior of the sample [24]. In addition, the orientation relation between the three phases at the interior of LENSed samples was obtained as 0001>Al2O3 // 001>YAG // 001>ZrO2 (with a slight deviation of 3.5°

between 001YAG with 11-20Al2O3 and 001ZrO2 obtained using Transmission Kikuchi Diffraction (TKD) technique and verified with High-resolution Transmission Electron Microscopy (HRTEM) imaging of a triple junction formed between Al2O3, YAG and ZrO2 phases (Fig. 3) [ The aforementioned difference could be explained by a conflict between growth kinetics and interfacial energy [24]. For instance, a better parallel nature of 11-20 Al2O3 //001 ZrO2 in comparison to that of 11-20 Al2O3//001 YAG [16], [24] may be the cause of the lower interfacial energy of Al2O3/ZrO2 interface ( 0.74 J/m2) as compared to that for Al2O3/YAG interface with an interfacial energy of 3.23 J/$m^2$ [24].

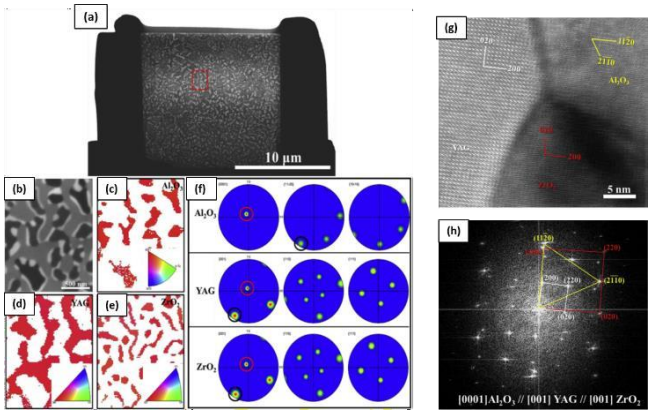


Fig. 3 AYZ shows the following images: (a) SEM image of the electron transparent lamella of the transverse section of the LENSed specimen created using the Focused Ion Beam (FIB)-based liftout technique; (b) SEM image of the region of interest for TKD mapping inside the cellular eutectic; (c), (d), and (e) TKD-based inverse pole figure (IPF) maps of Al2O3, A closer look at the area that was highlighted using a red-dotted rectangle in part **(a)** has been shown in part **(b)**.

A longitudinal segment of an LENSed AYZ specimen that was subjected to TKD analysis along BD is shown in Fig. 4 by means of a SEM picture [24]. The cellular eutectics' growth direction, which is 0001>Al2O3 // 001>YAG // 001>ZrO2 [24], is the same as that for the transverse section of AYZ samples. The longitudinal section, in contrast to the transverse section, also reveals YAG crystals with modest growth direction as 111> [24]. This may be explained by the fact that these crystals (which are primarily seen around cellular borders as shown in Fig. 4) deviated from their habit planes and then headed in that direction rather than continuing parallel to the direction of cell expansion. Sayir and Farmer [25] and Milenkovic [26] both reported a similar observation for the cellular eutectic Al2O3-ZrO2 and Ni-Al-V alloys, respectively.

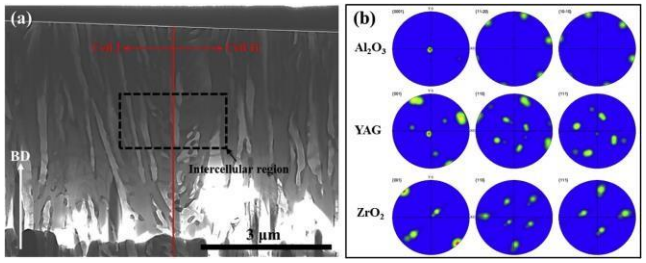

Fig. 4 AYZ shows (a) a SEM picture of the electron transparent lamella of the longitudinal slice of the LENSed specimen created utilising the TKD-based Focused Ion Beam (FIB)-based liftout approach, and (b) the pole figures of -Al2O3, -YAG, and -ZrO2 [24]. In part (a), a block-dotted rectangular box encloses the intercellular region from which the pole figures in part (b) were derived. BD abbreviates for building direction in section (a).

## 3. Future directions

The current state of research in the area of laser AM-based AZ ceramics has been briefly highlighted in the current article. The current goal (in this direction) is to tailor the microstructure (based on optimising a number of process parameters related to AM-based manufacturing techniques) to make these ceramics mechanically superior to those made using conventional methods. Characterization of the various interfaces, principally the eutectic boundaries in the current context, has not yet been addressed in the context of eutectic ceramics (particularly AZ ceramics). For instance, the case study discussed in section 4 is the only work (to date) that has been successfully able to use FIB-based liftout technique for obtaining electron transparent lamella from both transverse and longitudinal sections in AYZ ceramic in order to determine the orientation relationship between the individual phases (-Al2O3, YAG, and ZrO2) using TKD technique. This is true for both laser AM-based AZ ceramics and other laser-based materials.

Grain boundary engineering (GBE) of both metallic and ceramic materials has developed over the past forty years as a technique to optimise the various properties of these materials based on the substitution of high-energy random high-angle GBs (HAGBs) with low-energy GBs [27], [28]. GBE has been described as a mechanism to substitute regular HAGBs with special HAGBs (with low energy), also known as Coincidence Site Lattice (CSL) boundaries [29]–[32], which are more common in metallic materials with cubic crystal structures. The entire GBE methodology is built on lowering the total GB energy within a microstructure in order to make the 2D interfaces (GBs and IBs) resistant to corrosive, oxidising, irregular grain development, and intergranular fracture. Additionally, thermo-mechanical processing (TMP) is the most popular technique for producing GBE microstructures in most metallic materials [33]. Because the CSL theory does not work in the setting of ceramics with more intricate crystal structures, it is difficult to imagine the presence of low-energy CSL barriers [34]–[36]. Furthermore, due to their low deformability at both room and increased temperatures, ceramics preclude the employment of the procedures (particularly TMP) utilised to generate GBE microstructures in metallic materials. Consequently, creating GBE microstructures in AZ ceramics is quite difficult.

## 4. Summary and conclusion

Correlative Microscopy [37], [38] is one of the most recently developed approaches for linking the structure of GBs and interphase barriers (IBs) with their local atomic-scale composition (in polycrystalline materials). This methodology has been extensively used, especially in the context of metallic materials, to explore the structure and composition of GBs as well as the five macroscopic and three microscopic degrees of freedom(DOFs) (of GBs and IBs). There hasn't been much research into correlating microstructures in the context of AZ ceramics, though. The intricacy of crystal structures and sample preparationmay be the reason for this.

Furthermore, layer-by-layer material deposition is the foundation of laser AM-based processes, as indicated in section 1. By causing large-scale microstructural heterogeneities (with high defect concentration) [39] and non-equilibrium microstructures, this increases the complexity (in terms of creating GBE microstructures). As a result, the ability to generate GBE microstructures in AM-based AZ ceramics opens up a vast amount of possibilities for subsequent AZ ceramics research.


## Acknowledgement

MS is thankful to his undergraduate research supervisor Dr. Manab Mallik, Assistant Professor, Department of Metallurgical and Materials Engineering, NIT Durgapur, for detailed discussions during the scripting of the article.


## References


[1] J. M. Pappas, A. R. Thakur, and X. Dong, "Effects of zirconia doping on additively manufactured alumina ceramics by laser direct deposition," *Mater Des*, vol. 192, p. 108711, Jul. 2020, doi: 10.1016/j.matdes.2020.108711.

[2] V. K. Balla, S. Bose, and A. Bandyopadhyay, "Processing of bulk alumina ceramics using laser engineered net shaping," *Int J Appl Ceram Technol*, vol. 5, no. 3, pp. 234–242, May 2008, doi: 10.1111/j.1744-7402.2008.02202.x.

[3] C. K. Chua, K. F. Leong, and J. An, "Additive Manufacturing and 3D Printing," in *Biomedical Materials*, Springer International Publishing, 2021, pp. 621–652. doi: 10.1007/978-3-030-49206-9_19.

[4] O. Abdulhameed, A. Al-Ahmari, W. Ameen, and S. H. Mian, "Additive manufacturing: Challenges, trends, and applications," *Advances in Mechanical Engineering*, vol. 11, no. 2, Feb. 2019, doi: 10.1177/1687814018822880.

[5] Saha M, Mallik M. Surface engineering of nanomaterials: Processing and applications. InSurface Engineering 2022 Sep 14 (pp. 95-119). CRC Press

[6] M. Saha and M. Mallik, "Additive Manufacturing and Characterisation of Biomedical Materials," *Advanced Materials for Biomechanical Applications*, pp. 29–57, May 2022, doi: 10.1201/9781003286806-3.

[7] M. Saha and M. Mallik, "Metal-based conducive nano-inks: synthesis and characterization techniques," *Smart Multifunctional Nano-Inks*, pp. 27–52, Jan. 2023, doi: 10.1016/B978-0-323-91145-0.00003-7.

[8] M. Saha, "3D printing of nanoceramics: Present status and future perspectives," Sep. 2022, doi: 10.48550/arxiv.2210.06948.

[9] M. Saha, "Fly ash composites: A review," Feb. 2022, doi: 10.48550/arxiv.2202.11167.

[10] M. Saha, "Grain boundary segregation in steels: Towards engineering the design of internal interfaces," Feb. 2022, doi: 10.48550/arxiv.2202.12971.

[11] M. Saha, "New frontiers in characterising ZrB$_2$-MoSi$_2$ ultra-high temperature ceramics," Feb. 2022, doi: 10.48550/arxiv.2202.11162.

[12] M. Saha, “On the advanced microstructural characterisation of additively manufactured alumina-zirconia based eutectic ceramics: Overview and outlook,” Dec. 2022, doi: 10.26434/CHEMRXIV-2022-84LD6.

[13] W. E. Frazier, “Metal additive manufacturing: A review,” *Journal of Materials Engineering and Performance*, vol. 23, no. 6. Springer New York LLC, pp. 1917–1928, 2014. doi: 10.1007/s11665-014-0958-z.

[14] A. Zocca, P. Colombo, C. M. Gomes, and J. Günster, “Additive Manufacturing of Ceramics: Issues, Potentialities, and Opportunities,” *Journal of the American Ceramic Society*, vol. 98, no. 7, pp. 1983–2001, Jul. 2015, doi: 10.1111/jace.13700.

[15] A. Vyatskikh, S. Delalande, A. Kudo, X. Zhang, C. M. Portela, and J. R. Greer, “Additive manufacturing of 3D nano-architected metals,” *Nat Commun*, vol. 9, no. 1, pp. 1–8, Dec. 2018, doi: 10.1038/s41467-018-03071-9.

[16] M. Saha and M. Mallik, “Additive manufacturing of ceramics and cermets: present status and future perspectives,” *Sādhanā 2021 46:3*, vol. 46, no. 3, pp. 1–35, Aug. 2021, doi: 10.1007/S12046-021-01685-2.

[17] F. Li and Y. Zhang, “ Microstructural characterization of Al 2 O 3 -ZrO 2 ceramic by laser direct material deposition ,” *J Laser Appl*, vol. 31, no. 2, p. 022509, May 2019, doi: 10.2351/1.5096125.

[18] J. Wilkes, Y. C. Hagedorn, W. Meiners, and K. Wissenbach, “Additive manufacturing of ZrO2-Al2O3 ceramic components by selective laser melting,” *Rapid Prototyp J*, vol. 19, no. 1, pp. 51–57, 2013, doi: 10.1108/13552541311292736.

[19] J. Homeny and J. J. Nick, “Microstructure-property relations of alumina-zirconia eutectic ceramics,” *Materials Science and Engineering A*, vol. 127, no. 1, pp. 123–133, Jul. 1990, doi: 10.1016/0921-5093(90)90198-C.

[20] J. M. Calderon-Moreno and M. Yoshimura, “Stabilization of zirconia lamellae in rapidly solidified alumina-zirconia eutectic composites,” *J Eur Ceram Soc*, vol. 25, no. 8 SPEC. ISS., pp. 1369–1372, Jan. 2005, doi: 10.1016/j.jeurceramsoc.2005.01.013.

[21] V. Trnovcovfi, M. Starostin, V. Labas, and R. Cicka, “Microstructure and Physical Properties of Directionally Solidified Alumina-Zirconia Eutectic Composites,” 1998.

[22] H. Liu *et al.*, “One-step additive manufacturing and microstructure evolution of melt-grown Al2O3/GdAlO3/ZrO2 eutectic ceramics by laser directed energy deposition,” *J Eur Ceram Soc*, vol. 41, no. 6, pp. 3547–3558, Jun. 2021, doi: 10.1016/j.jeurceramsoc.2021.01.047.

[23] H. Liu *et al.*, “Effect of scanning speed on the solidification process of Al2O3/GdAlO3/ZrO2 eutectic ceramics in a single track by selective laser melting,” *Ceram Int*, vol. 45, no. 14, pp. 17252–17257, Oct. 2019, doi: 10.1016/j.ceramint.2019.05.281.

[24] Z. Fan *et al.*, “Nanostructured Al 2 O 3 -YAG-ZrO 2 ternary eutectic components prepared by laser engineered net shaping,” *Acta Mater*, vol. 170, pp. 24–37, May 2019, doi: 10.1016/j.actamat.2019.03.020.

[25] A. Sayir and S. C. Farmer, “Effect of the microstructure on mechanical properties of directionally solidified Al2O3/ZrO2(Y2O3) eutectic,” *Acta Mater*, vol. 48, no. 18–19, pp. 4691–4697, Dec. 2000, doi: 10.1016/S1359-6454(00)00259-7.

[26] S. Milenkovic, A. A. Coelho, and R. Caram, “Directional solidification processing of eutectic alloys in the Ni-Al-V system,” *J Cryst Growth*, vol. 211, no. 1, pp. 485–490, Apr. 2000, doi: 10.1016/S0022-0248(99)00783-6.

[27] D. Raabe *et al.*, “Grain boundary segregation engineering in metallic alloys: A pathway to the design of interfaces,” *Curr Opin Solid State Mater Sci*, vol. 18, no. 4, pp. 253–261, 2014, doi: 10.1016/j.cossms.2014.06.002.

[28] Y. Ikuhara, “Grain boundary and interface structures in ceramics,” *Journal of the Ceramic Society of Japan*, vol. 109, no. 1271. Ceramic Society of Japan, pp. S110–S120, Jul. 01, 2001. doi: 10.2109/jcersj.109.1271_S110.

[29] A. D. Rollett, “Texture development dependence on grain boundary properties,” in *Materials Science Forum*, 2002, vol. 408–412, no. I, pp. 251–256. doi: 10.4028/www.scientific.net/msf.408-412.251.

[30] M. Winning and A. D. Rollett, “Transition between low and high angle grain boundaries,” *Acta Mater*, vol. 53, no. 10, pp. 2901–2907, Jun. 2005, doi: 10.1016/j.actamat.2005.03.005.

[31] D. Brandon, “25 Year Perspective Defining grain boundaries: An historical perspective the development and limitations of coincident site lattice models,” *Materials Science and Technology*, vol. 26, no. 7. pp. 762–773, Jul. 01, 2010. doi: 10.1179/026708310X12635619987989.

[32] D. G. Brandon, “The structure of high-angle grain boundaries,” *Acta Metallurgica*, vol. 14, no. 11, pp. 1479–1484, 1966, doi: 10.1016/0001-6160(66)90168-4.

[33] W. M. Ashmawi and M. A. Zikry, “Prediction of grain-boundary interfacial mechanisms in polycrystalline materials,” *Journal of Engineering Materials and Technology, Transactions of the ASME*, vol. 124, no. 1, pp. 88–96, 2002, doi: 10.1115/1.1421611.

[34] V. Y. Gertsman, A. P. Zhilyaev, and J. A. Szpunar, “Grain boundary misorientation distributions in monoclinic zirconia,” *Model Simul Mat Sci Eng*, vol. 5, no. 1, pp. 35–52, Jan. 1997, doi: 10.1088/0965-0393/5/1/003.

[35] H. Grimmer, “Coincidence-site lattices,” *Acta Crystallographica Section A*, vol. 32, no. 5, pp. 783–785, Sep. 1976, doi: 10.1107/S056773947601231X.

[36] A. P. Sutton, R. W. Balluffi, and V. Vitek, “On intrinsic secondary grain boundary dislocation arrays in high angle symmetrical tilt grain boundaries,” *Scripta Metallurgica*, vol. 15, no. 9, pp. 989–994, 1981, doi: 10.1016/0036-9748(81)90240-4.

[37] Y. Toji, H. Matsuda, M. Herbig, P. P. Choi, and D. Raabe, “Atomic-scale analysis of carbon partitioning between martensite and austenite by atom probe tomography and correlative transmission electron microscopy,” *Acta Mater*, vol. 65, pp. 215–228, Feb. 2014, doi: 10.1016/j.actamat.2013.10.064.

[38] C. H. Liebscher *et al.*, “Tetragonal fcc-Fe induced by κ -carbide precipitates: Atomic scale insights from correlative electron microscopy, atom probe tomography, and density functional theory,” *Phys Rev Mater*, vol. 2, no. 2, pp. 1–6, 2018, doi: 10.1103/PhysRevMaterials.2.023804.

[39] M. Schwentenwein and J. Homa, “Additive manufacturing of dense alumina ceramics,” *Int J Appl Ceram Technol*, vol. 12, no. 1, pp. 1–7, Jan. 2015, doi: 10.1111/ijac.12319.